Wind Gust and Turbulence Statistics of Typhoons in South China*

WANG Binglan[1,2](王丙兰), HU Fei[1†](胡 非), and CHENG Xueling[1](程雪玲)

1 *LAPC, Institute of Atmospheric Physics, Chinese Academy of Sciences, Beijing* 100029

2 *Graduate University of Chinese Academy of Sciences, Beijing* 100049

(Received May 20, 2010; in final form October 9, 2010)

ABSTRACT

The wind data of four typhoons were obtained and analyzed. The wind speeds were measured by sonic anemometers at four observation sites in Guangdong and Hainan provinces. Detailed analysis of the wind data was conducted to investigate the turbulence characteristics of the typhoons. Characteristics of the gust factor and the turbulence integral scale of the typhoons were concluded with high confidence. The relationships among the gust factor, gust duration time, mean wind speed, roughness length, and turbulence intensity were described. The turbulence integral scale was found to be closely related to the segment length and turbulence intensity.

Key words: gust factor, turbulence integral scale, typhoon

Citation: Wang Binglan, Hu Fei, and Cheng Xueling, 2011: Wind gust and turbulence statistics of typhoons in South China. *Acta Meteor. Sinica*, **25**(1),113–127, doi: 10.1007/s13351-011-0009-8.

1. Introduction

As one of the most destructive and disasterous weathers, the typhoon involving heavy rain or strong wind exerts considerable adverse effects on people's life and the economy. Therefore, analysis of typhoon characteristics is of great significance in both the wind engineering and meteorological studies. Researches on typhoons have been performed in many years. Powell (1982) studied the wind field of Hurricane Frederic that struck Gulf Coast, with aircraft, ship, buoy, and land station data. Zhou et al. (2003) made numerical simulations of the developing process of two cyclones by using the MM5 mesoscale model. Jiang et al. (2008) studied the air-sea interaction during the life cycle of a typhoon and the quantificational effects of typhoon-induced sea surface temperature (SST) cooling on typhoon intensity, using a mesoscale coupled air-sea model. Ming et al. (2009) analyzed the dynamical characteristics and wave structure of Typhoon Rananim. Li et al. (2009) investigated the eyewall evolution of Typhoon Imbudo by using the MM5 model. Yuan et al. (2009) analyzed the temporal and spatial variations of tropical cyclones (TCs) on different intensity scales. Zhao et al. (2009) performed numerical simulations of a heavy rainfall event triggered by an inverted typhoon trough using the non-hydrostatic mesoscale model MM5.

However, in terms of the turbulence characteristics of the typhoon, existing investigations seem to be inadequate due to the lack of field measurements. In fact, turbulent fluctuations and gusts in high winds are critical factors that impact wind loads (Floris and Iseppi, 1998; Harikrishna et al., 1999; Hui et al., 2009). Wind tunnel experiments and numerical simulations of intensive wind gusts associated with turbulence have been well developed (Kobayashi et al., 1994; Brasseur, 2001; Goyette et al., 2003). Shiau (2000) discussed the characteristics of typhoon turbulence on the northeastern coast of Taiwan, using data from the three-axis ultra-sonic anemometer. Miyata et al. (2002) analyzed the effects of 9807 and 9918 typhoons on Akashi Kaikyo Bridge in Japan, using full-scale measurement data from anemometers, accelerometers, thermometers, and GPS sensors.

Humid and mild marine climate exists in southern coastal regions of China, such as Guangdong and Hainan provinces However, every summer, several

*Supported by the National Natural Science Foundation of China under Grant Nos. 90715031, 40775018, and 40875008, and the National Science & Technology Pillar Program under Grant No. 2008BAC37B00.

†Corresponding author: hufei@mail.iap.ac.cn.

typhoons land in these regions, causing severe damage to tall buildings and bridges. As turbulent fluctuations and gusts in high winds are important factors that determine the wind loads, it is necessary to analyze the turbulence structure of a typhoon in order to provide reference for design and risk evaluation of tall buildings. In this study, high resolution data of four selected typhoons (Washi, Damrey, Chanchu, and Prapiroon) were obtained from different sites in South China. Based on the data, a detailed analysis of gust factors and turbulence integral scales was performed. The characteristics of the gust factor and integral scale associated with typhoon passages in southern China were identified.

2. Data sources

Wind data used in this paper are collected from four observation sites during four typhoon passages that struck South China in 2005 and 2006. The information about the observation sites is shown in Table 1 and Fig. 1. At all the four observation sites, HD2003 ultra-sonic anemometers were installed at 10-m (or 12-m) height. The recording and processing of the turbulence data were carried out on a notebook PC based on the same data acquisition system at the four sites. With the sampling frequency of 1 Hz, it is reasonable to evaluate the gust factor and turbulence integral length scales of typhoon winds.

Table 1. Observation sites for four typhoons

Name	Observation site	Anemometer height	Location	Observation period (UTC)
Washi	Wenchang, Hainan	10 m	19.54°N, 110.80°E	0000–1200 UTC 30 Jul. 2005
Damrey	Xuwen, Guangdong	12 m	20.42°N, 110.18°E	0300–2200 UTC 26 Sep. 2005
Chanchu	Raoping, Guangdong	10 m	23.66°N, 116.99°E	0200–1500 UTC 17 May 2006
Prapiroon	Maoming, Guangdong	10 m	21.48°N, 111.02°E	1300 UTC 3 Oct.–0100 UTC 4 Oct. 2006

All the data were pre-processed in the following steps:

(1) Finding the turbulence data spikes. According to the methods of HØjstrup (1993) and Vickers and Mahrt (1997), spikes are identified based on the following formula:

$$|\mathrm{d}x(i)| = 3\sigma, \tag{1}$$

where x represents the series of u, v, and $w, \mathrm{d}x(i) = x(i+1) - x(i)$, and σ is the standard deviation of series x.

(2) Removing and interpolating the spikes by using the HØjstrup (1993) method:

$$x(i) = x(i-1)R_m + (1 - R_m)X_m, \tag{2}$$

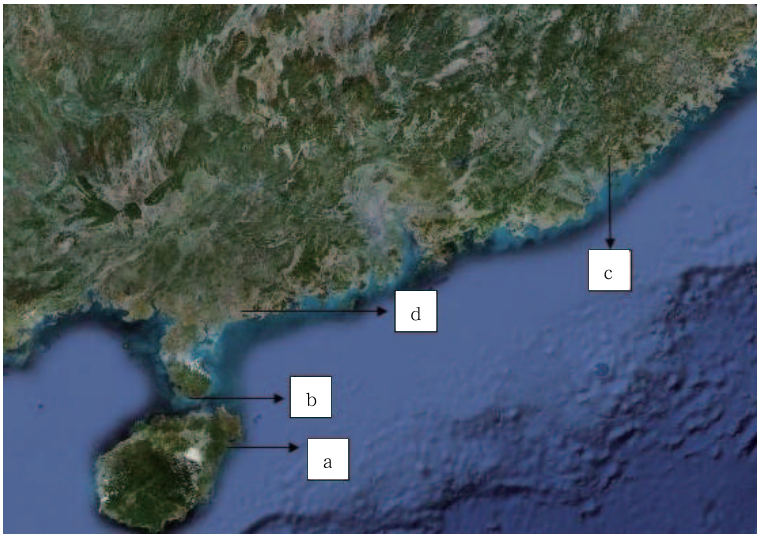

Fig. 1. Observation sites and corresponding typhoons. The letters a–d denote Typhoon Washi, Damrey, Chanchu, and Prapiroon, respectively.

where m is a constant ($m = 10$ in this paper), R_m is the correlation coefficient between the series $x(i-m:i-3)$ and $x(i-m+2:i-1)$, and X_m is the mean of the series $x(i-m:i-1)$.

(3) Setting 8 m s^{-1} at 10-m (or 12-m) height as the minimum requirement for 10-min segment mean wind speed. This approximately satisfies the condition of strong wind and neutral stability.

Moreover, according to Zhang et al. (2001), the 10-min runs were rejected if 1) the angle between the horizontal wind direction and the coordinate system of the sonic anemometer is greater than 45°, and 2) the slope angle between the vertical and horizontal components of the wind is greater than 3°. A statistical summary of the typhoon wind speeds is shown in Table 2.

Table 2. Summary of the observed typhoons

Name		Washi	Damrey	Chanchu	Prapiroon
Numbers of 10-min segments		71	114	78	71
Mean wind speed (m s^{-1})	Min	10.5	9.0	8.8	13.0
	Max	19.9	25.7	23.4	25.4
	Mean	14.1	17.9	16.8	16.8
	Std	2.2	5.1	3.6	2.0
Roughness length (m)	Min	0.0008	0.0004	0.0065	0.0006
	Max	0.1496	0.1335	0.3127	0.0632
	Mean	0.0511	0.0329	0.0679	0.0176
	Std	0.0417	0.0381	0.0525	0.0128
2-s/10-min gust factor	Min	1.22	1.24	1.34	1.21
	Max	1.67	1.58	2.10	1.44
	Mean	1.40	1.38	1.57	1.32
	Std	0.12	0.09	0.14	0.05

3. Results

3.1 Roughness length

There are several methods to determine the roughness length z_0, based on the log-law wind profile under neutral conditions:

$$U = \frac{u_*}{k}\ln\Big(\frac{z}{z_0}\Big), \tag{3}$$

where u_* is the friction velocity, k is the Von-Karman constant, which is usually set to be 0.4, z is the anemometer height, and U is the mean wind speed at z height.

Considering the applicability of Eq. (3) for typhoons, Wieringa (1976) suggested that Eq. (3) can be used to estimate the mean wind speed of a typhoon when the wind speed is greater than 6 m s^{-1}. Meanwhile, Sharma and Richards (1999) concluded that TC winds are convectively unstable, but the difference between TC profile and neutral profile is very small below the height of 10 m. Since the height here is about 10 m and the 10-min mean wind speed is higher than 8 m s^{-1} (see Table 2), Eq. (3) is applicable.

The roughness length z_0, involved in the intercept of the semi-log plot of U and z, can be obtained when data from multiple anemometer heights are available. Otherwise, z_0 is directly estimated from Eq. (3) using high resolution data, with the friction velocity obtained by

$$u_*^2 = \sqrt{\overline{u'w'}^2 + \overline{v'w'}^2}, \tag{4}$$

where u', v', and w' are the longitudinal, lateral, and vertical fluctuation components of wind, respectively. Another widely used method in typhoon analysis is called the turbulence intensity (TI) method, which is based on the analysis of the standard deviation of the horizontal component of the wind (Beljaars, 1987). Sozzi et al. (1998) and Letchford et al. (2001) applied the following similarity equation

$$\frac{\sigma_u}{u_*} = 2.5. \tag{5}$$

By substituting Eq. (5) into Eq. (3), we obtain

$$z_0 = \exp(\ln(z) - \frac{1}{I}), \tag{6}$$

where I is the TI. This expression can be used to calculate z_0.

Figure 2a shows the roughness length z_0 calculated by using the above two different methods. Obviously, the values of z_0 obtained from Eq. (3) from high resolution data (the direct method) are much smaller than those from the TI method. This may be caused by the uncertainties in the estimation of u_* using conventional friction velocity measurements (Johnson et al., 1998).

For better analysis and interpretation of turbulence statistics over surfaces with different roughness characteristics, the method of roughness classification has been widely used (Schroeder et al., 2002, Paulsen and Schroeder, 2005). By using the roughness lengths calculated from the TI method, the dataset is stratified into four roughness regimes: smooth, open, open to roughly open, and roughly open to rough. Table 3 lists the roughness regimes and associated roughness length. This method is also employed to find out the distribution of the 10-min roughness length z_0 calculated from the TI method for the four selected typhoons. The results are shown in Fig. 2b. Evidently, most of the z_0 values are in the regimes presented in Table 3. The roughness length lower than 0.0050 makes up a large portion of white roughness length, which is not included in regimes of Schroeder et al. (2002). Roughness length in the range of 0–0.0049 is defined as the sea regime in Table 3 according to Wieringa (1992) and Schroeder et al. (2002). It should be noted that the sea regime is just one of names of the roughness regimes, and does not refer to the real sea surface.

Table 3. Roughness regimes and associated roughness lengths

Roughness	Roughness length (m)
Sea	0 –0.0049
Smooth	0.0050 –0.0199
Open	0.0200 –0.0499
Open to roughly open	0.0500 –0.0899
Roughly open to rough	0.0900 –0.1899

The 10-min roughness length calculated from the TI method is given in Table 2. The smallest mean and standard deviation of the roughness length appear with Typhoon Prapiroon, indicating the smoothest upstream terrain conditions.

3.2 Gust factor

The gust factor is defined as the ratio of the maximum wind speed in duration t to the wind speed averaged over period T. It is given as

$$G_{t,T} = \frac{u_{\max,t}}{\overline{u_T}}, \tag{7}$$

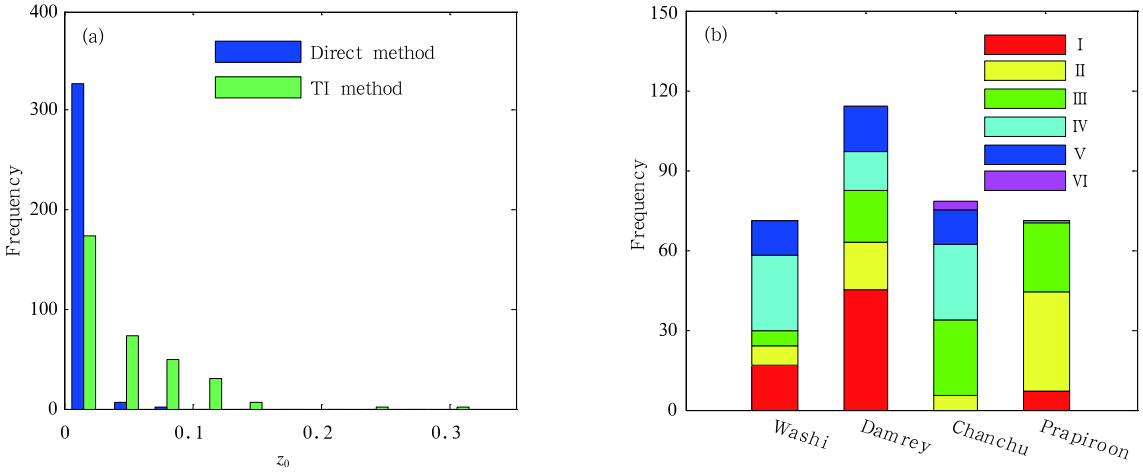

Fig. 2. (a) Histogram of roughness length z_0 calculated by the direct method and the TI method. (b) Histogram of roughness regimes for different typhoons, with I–VI denoting regimes of sea, smooth, open, open to roughly open, roughly open to rough, and $z_0 > 0.1899$ m, respectively.

where $u_{\max,t}$ is the maximum of the running average wind speed over t seconds and $\overline{u_T}$ is the wind speed averaged over T seconds.

The gust factor is affected by various elements such as stability of the boundary layer, anemometer height, and upstream terrain conditions (roughness length). It is usually greater for tropical storms than for monsoon winds (Choi and Hidayat, 2002). In recent years, the research on gust characteristics has made significant progress. Choi (1999) found that the gust factor during thunderstorms becomes higher in Singapore. Nielsen and Petersen (2001) analyzed the gust factor in different atmospheric stable stratification conditions by applying the similarity theory. Hsu (2003) presented the relationship between the gust factor G and the exponent of the power-law wind profile P. Hsu and Blanchard (2004) implied that the TI is linearly related to the gust factor under neutral and stable conditions over the sea surface. Jungo et al. (2002) categorized 10-yr Swiss station observations into three weather types over Switzerland and derived daily wind gust speed probabilities using the gust factor. Vickery and Skerlj (2005) revised the gust factor for a hurricane, suggesting that in most cases, gust factor for the hurricane can be described by models developed for standard neutral boundary layer flow conditions.

In this section, relations between the gust factor and several variables such as gust duration, mean wind speed, roughness length, and turbulence intensity are investigated. Table 2 gives a statistical summary of the 2-s/10-min (that is, $t = 2$ s, $T = 10$ min) gust factor based on the data from four different deployment locations with different roughness lengths. The gust factors ranging from 1.21 in Typhoon Prapiroon to 2.10 in Typhoon Chanchu seem to be sensitive to the roughness length.

3.2.1 Gust factor and gust duration

No standard exists for selection of gust duration t and averaging period T of the mean wind speed. To calculate wind load, Faber and Bell (1963) recommended setting $t = 1$ min and $T = 60$ min to calculate the gust factor for a building as a whole, and $t = 10$ s for building details, while Harstveit (1996) used $t = 3$ s and $T = 10$ min to clarify the relationship between the gust factor and TI. Mitsuta (1962) first proposed the following formula to describe the relation between the gust factor and gust duration.

$$G = \left(\frac{t}{T}\right)^{-p}, \tag{8}$$

where p is a constant depending on the roughness condition.

Assuming the averaging period $T = 600$ s, the gust factor can be calculated by using Eq. (7). Figure 3 shows the variation of the gust factor with gust duration based on the data classified by the roughness regime on the semi-logarithmic scale.

It is clear to see that (1) for the same roughness regime, the gust factor decreases approximately linearly with gust duration t on the semi-logarithmic scale. (2) For the same gust duration time t, the rougher the surface (e.g., terrain), the greater the gust factor. (3) The constant p increases gradually from 0.123 in the sea regime to 0.219 in the roughly open to rough regime, indicating that p is sensitive to terrain condition, or the roughness length.

3.2.2 Gust factor and average wind speed

Davis and Newstein (1968) reported a linear relation between the peak gust and the corresponding mean wind speed, using the observational data from a 1000-ft (about 305-m) tower:

$$U_{\max} = aU + b, \tag{9}$$

where a and b are empirical constants. By substituting Eq. (9) to Eq. (7), the expression of the gust factor G is obtained:

$$G = \frac{U_{\max}}{U} = a + b/U \tag{10}$$

A scatter plot of the 2-s/10-min gust factor (that is, $t = 2$ s and $T = 10$ min) vs. mean wind speed for the four selected typhoons shown in Fig. 4 demonstrates that the gust factor decreases with the increase of mean wind speed. The green circles in Fig. 4, which denote Typhoon Damrey, show the reciprocal relation between the gust factor and the mean wind speed as described in Eq. (10).

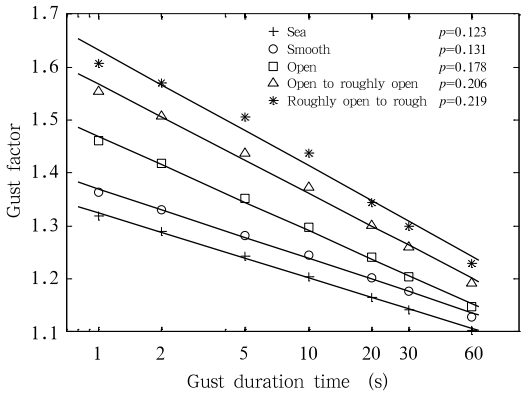

Fig. 3. Gust factor as the function of the gust duration time.

It is interesting to see that the gust factor varies slightly when the mean wind speed is higher than a certain value. According to Eq. (10), the gust factor would not change if the mean wind speed was higher than a certain value (such as 14 m s^{-1} in Mitsuta and Tsukamoto (1989)). For Typhoon Prapiroon with a relative smooth and homogeneous upstream terrain condition, the critical value of 14 m s^{-1} is practicable. But for the other three typhoons (Washi, Damrey, and Chanchu), the critical value should be larger than 14 m s^{-1}.

For every selected typhoon, the range of the gust factor is different. The gust factor range for Typhoon Prapiroon is the smallest, only about 0.2, while the gust factor ranges of the other three typhoons are all about 0.4. The difference of gust factor ranges among different typhoons could be attributed to different roughness characteristics, which will be discussed in the next section.

3.2.3 Gust factor and roughness length

Owing to the sensitivity of the gust factor to the surrounding terrain condition, roughness must be considered when the gust factor is determined. Krayer and Marshall (1992) estimated that the gust factor with the surface roughness length $z_0 = 0.03$ m is about 1.55. They used wind speed strip chart records collected from four different hurricanes. Through analysis of the high-resolution wind speed data gathered from Hurricane Bonnie in the Wind Engineering Mobile Instrumented Tower Experiment (WEMITE), Schroeder and Smith (2003) revealed the linear relationship between the gust factor and roughness length, described by

$$G = cz_0 + d. \tag{11}$$

This is derived from the least square fitting method.

As shown in Table 2, the mean gust factors are different for different typhoons. It seems that the gust factor increases with roughness length. The scatter plots of the 2-s/10-min gust factor vs. roughness length for the four selected typhoons shown in Fig. 5 further illustrate that the gust factor increases approximately linearly with roughness length. The values of slope c in Eq. (11) for the four typhoons are 2.31, 1.89,

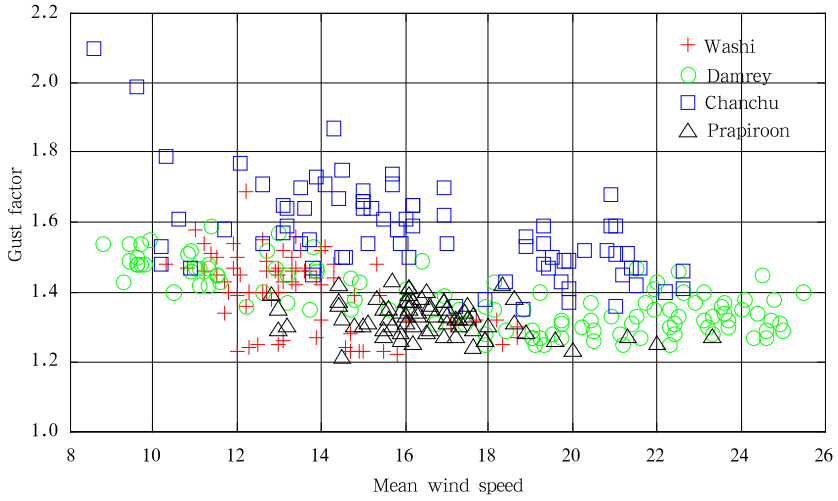

Fig. 4. Scatter plot of the gust factor vs. mean wind speed.

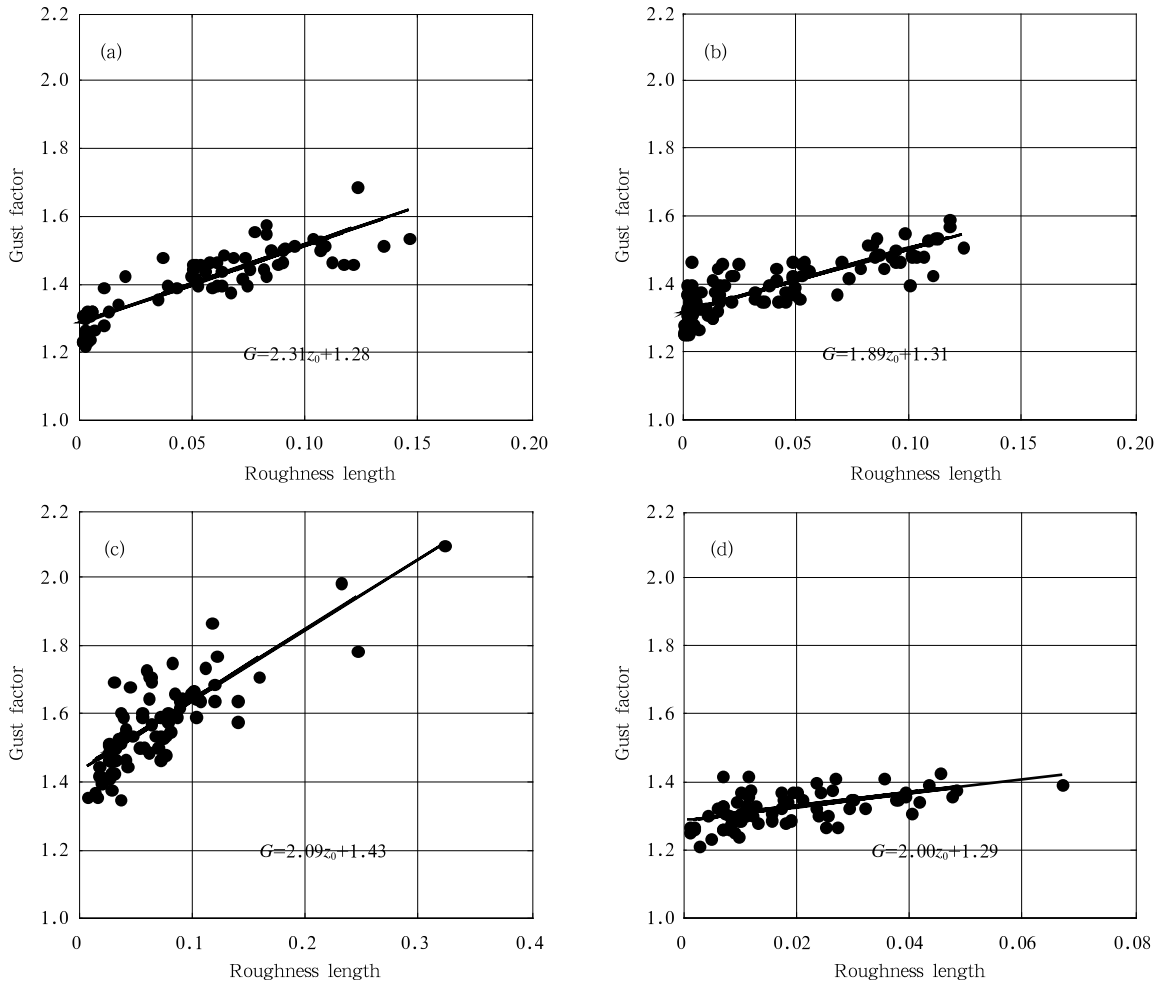

Fig. 5. Scatter plots of the gust factor vs. roughness length for Typhoon (a) Washi, (b) Damrey, (c) Chanchu, and (d) Prapiroon.

2.09, and 2.00, respectively. The difference may result from the difference in mean wind speed. As shown in Table 2, the mean wind speeds of these typhoons are 14.1, 17.9, 16.8, and 16.8, respectively. It seems that the lower wind speed corresponds to the higher value of c, i.e., the gust factor increases faster at the lower wind speed.

Based on Eq. (11), and with the roughness set length as 0.03 m, the gust factors for the four typhoons are estimated as 1.35, 1.37, 1.49, and 1.35, respectively, smaller than the value of 1.55 from Krayer and Marshall (1992). Since the gust factor is evaluated under the same conditions: the same roughness length ($z_0 = 0.03$ m), the same anemometer height (z is about 10 m), and the same t and T (t= 2 s and T = 600 s), the underestimation of the gust factor may result from the high mean wind speed (most of which are higher than 10 m s^{-1}). In contrast, the wind speed of a significant portion of the hurricanes examined by Krayer and Marshall (1992) is lower than 10 m s^{-1}. As discussed in Section 3.2.1, the gust factor decreases with the increase of mean wind speed. Therefore, the gust factors of the four typhoons with higher wind speeds are smaller than those from Krayer and Marshall (1992) even though the roughness length is the same.

As pointed out in Section 3.2.1, the gust factor ranges (ΔG) change with the roughness condition. This can be easily explained by using Eq. (11), which is followed by

$$\Delta G = c\Delta z_0. \tag{12}$$

Obviously, assuming the same slope c, a larger Δz_0 corresponds to a larger ΔG. As shown in Fig. 5 and Table 2, the smallest Δz_0 (about 0.0626) comes with Typhoon Prapiroon, and the corresponding maximum z_0 is only 0.0632. The values of Δz_0 with the other three typhoons seem relatively large (about 0.15). Thus, considering nearly the same slopes for the four typhoons, ΔG of Typhoon Prapiroon with the smallest Δz_0 must be the smallest.

In order to further explain the relationship between the gust factor and roughness length, calculated roughness length values are used to stratify the data into various roughness regimes using the method proposed in Section 3.1. A scatter plot of the 2-s/10-min gust factor vs. mean wind speed is given in Fig. 6. We see that the gust factor changes slightly with mean wind speed, especially in smooth and open regimes. The gust factors for the sea, smooth, and open regimes are distributed into three distinct layers, but there is no obvious difference between open to roughly open regime and roughly open to rough regime. From bottom to top, the roughness of regimes increases with the increase of the gust factors and their ranges. Paulsen and Schroeder (2005) obtained a similar result using high resolution wind speed data (2–10 Hz) collected from both landfalling TCs and extratropical systems.

3.2.4 Gust factor and turbulence intensity

The relationship between the gust factor and TI has been studied for many years. Choi (1983) proposed that the gust factor G is proportional to $I^{1.27}$ based on the wind speed data measured in Hong Kong. This was supported by Xu and Zhan (2001) and Fu et al. (2008). The simplified expression used commonly is given by

$$G = 1 + \alpha I, \tag{13}$$

where I is turbulence intensity and α is the peak factor that may change in different events. Harstveit (1996) revealed that α values are grouped around 2.44±0.2. He used data recorded during strong winds from five exposed stations in inhomogenous and hilly terrain in Norway. Li et al. (2004) reported that the value of α was 2.21, based on field data measured from Di Wang Tower located in Shenzhen during the passage of Typhoon Sally in 1996. It should be pointed out that different values of gust duration t and average time T were selected by different researchers when the gust factor were calculated. This may result in different values of the peak factor.

Based on 10-min records, the gust factor and TI are calculated and plotted in Fig. 7. As expected, all points in this figure are distributed approximately on a straight line. The fitted formulas indicating the relationship between the gust factor and turbulence intensity are also shown in Fig. 7. The slopes of the straight lines, i.e., the peak factors of the four typhoons, are 2.28, 2.42, 2.96, and 2.09, respectively.

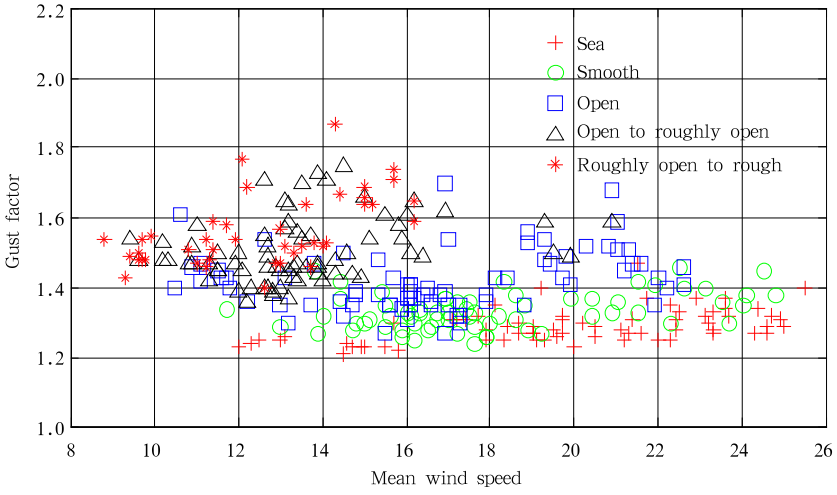

Fig. 6. Scatter plot of the gust factor vs. mean wind speed.

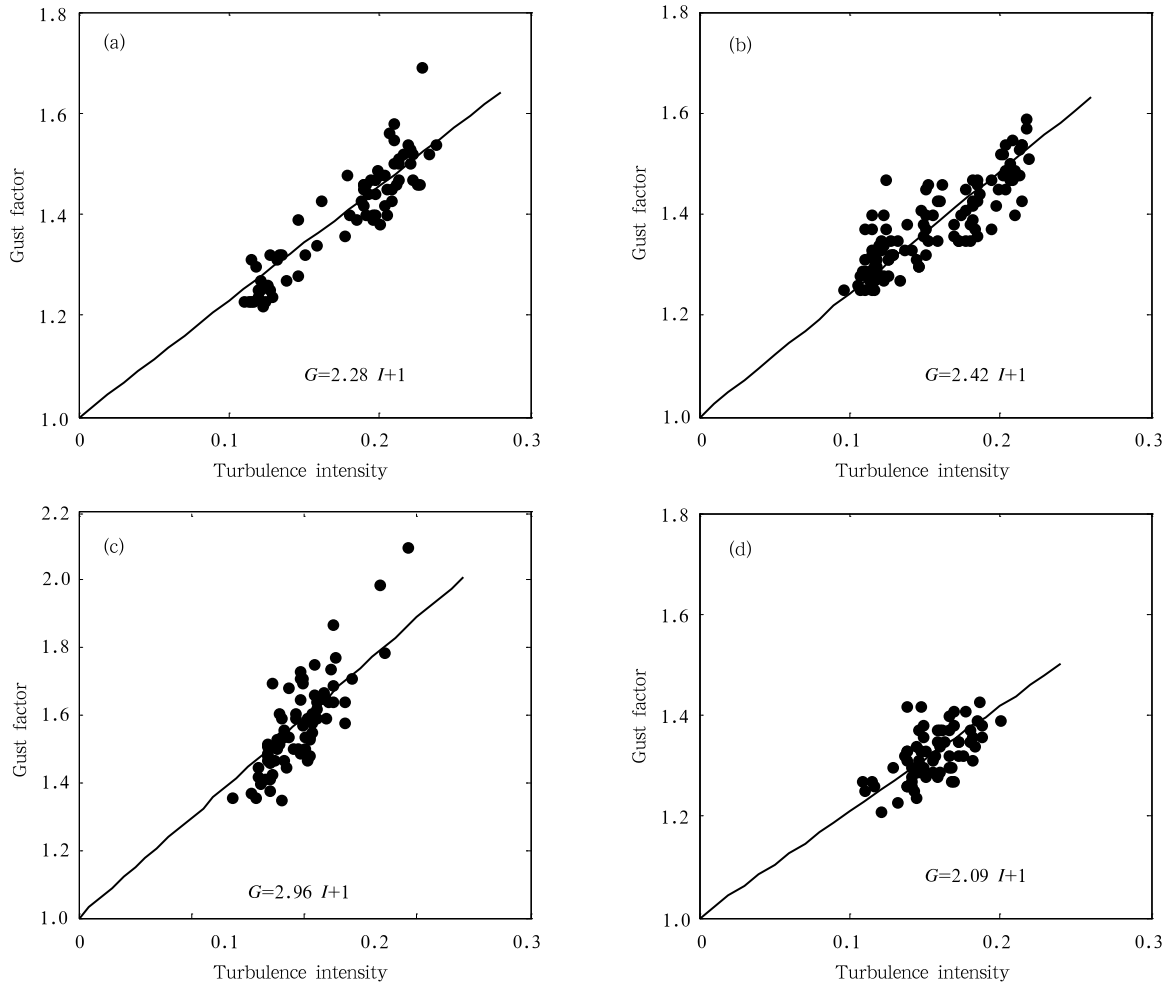

Fig. 7. Scatter plots of the gust factor vs. turbulence intensity for (a) Washi, (b) Damrey, (c) Chanchu, and (d) Prapiroon.

3.3 Turbulence integral length scale

Turbulence integral scale, a measure of the average size of the turbulent eddy of the flow, varies greatly in the atmospheric boundary layer. There are several methods to calculate the turbulence integral scale, which may give significantly different calculation results (Garg et al., 1997). Reed and Scanlan (1984) determined the integral scale from an autoregressive (AR) model. Kato et al. (1992) pointed that the longitudinal integral scale can be estimated from the power spectrum density function if the longitudinal fluctuation wind speed spectrum is consistent with the Von-Karman spectrum. Liu et al. (2003) calculated the turbulence integral scale by using the turbulence dissipation rate. The most commonly used method is to integrate the autocorrelation coefficient directly based on the definition of the integral scale.

The turbulence integral scale is defined as

$$L_i^M = \frac{1}{\sigma_i^2}\int_0^\infty R_{12}(M)\mathrm{d}M, \tag{14}$$

where $i = u, v, w$, $M = x, y, z$, andσ_i^2 is the variance of the wind component fluctuation. R_{12} is the covariance function between the fluctuating velocity $u_1(x_1, y_1, z_1, t_1)$ and $u_2(x_2, y_2, z_2, t_2)$. The longitudinal integral length scale L_u^x can be expressed as

$$L_u^x = \frac{1}{\sigma_i^2}\int_0^\infty R_{12}(M)\mathrm{d}M. \tag{15}$$

According to Taylor's frozen hypothesis, Eq. (15)

can be modified into

$$L_u^x = \frac{1}{\sigma_u^2}\int_0^\infty R_u(\tau)\mathrm{d}\tau = U\int_0^\infty \rho_{uu}(\tau)\mathrm{d}\tau, \qquad (16)$$

where U is the mean wind speed, and ρ_{uu} is the autocorrelation coefficient function of the longitudinal wind component, defined as:

$$\rho_{uu}(\tau) = \frac{E[\{u(t)-u\}\{u(t+\tau)-U\}]}{\sigma_u^2}, \qquad (17)$$

where $E[\varphi(t)]$ is the expected value of the stationary random process $\varphi(t)$. The expressions of lateral and vertical integral scales can then be obtained according to Eq. (14).

The turbulence integral scale in this paper is calculated by using Eq. (16). The autocorrelation coefficient ρ_{uu} must be first estimated in order to calculate the turbulence integral scale. Figure 8 shows the variation of the autocorrelation coefficient ρ_{uu} with lag time τ for different length segments (10, 30, and 60 min) for Typhoon Prapiroon. It is seen that, for the same lag time τ, the autocorrelation coefficient ρ_{uu} with 10-min segment is the smallest, while ρ_{uu} with 60-min segment is the largest. This indicates that the autocorrelation coefficient depends on the length of a segment.

According to Eq. (16), the upper limit of the integral is infinite. In practice, since Eq. (16) is obtained by applying Taylor's hypothesis, which may cause larger errors if the autocorrelation coefficient is too small, the upper limit of the integral is taken as 0.05, as suggested by Flay and Stevenson (1988).

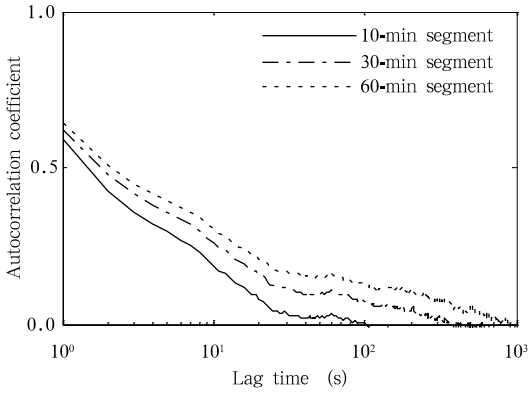

Fig. 8. Variation of autocorrelation coefficient with lag time for different segments in Typhoon Prapiroon.

Table 4 displays values of the turbulence integral scale for different segments of the four typhoons. It shows that: (1) for every typhoon, both the longitudinal and lateral integral length scales increase with the segment length. For Typhoon Damrey, the longitudinal integral length scale ranges from the smallest (210 m) for 5-min segmeant to the largest (875 m) for 60-min segment. (2) The 10-min longitudinal integral scales for the four typhoons are 134, 287, 286, and 169 m, which are within the range of 60–400 m obtained by Schroeder et al. (1998). (3) The relationship between L_u^x and L_v^x can be represented by their ratio. The ratio L_u^x/L_v^x obtained by Smedman et al. (1995) was about 2.5, while Cao et al. (2009) derived it to be about 2.4, based on 10-min wind speed samples from Typhoon Maemi. In this study, only the ratio L_u^x/L_v^x in Typhoon Damrey, with a value of 2.5, is comparable to their results. (4) The vertical integral scale, with significantly smaller values compared with the longitudinal and lateral ingegral scales, changes a little with segment length. (5) The integral scale varies from typhoon to typhoon. The ratio between the largest to the smallest integral scale for the 10-min segment is $287/134 \approx 2.14$, and $1105/678 \approx 1.63$ for the 60-min segment.

Table 4. Turbulence integral length scales

Integral scales (m)	Segment (min)	Washi	Damrey	Chanchu	Prapiroon
L_u^x	5	97	210	192	125
	10	134	287	286	169
	20	296	370	414	288
	30	361	488	532	499
	40	597	679	593	780
	60	1083	875	678	1105
L_v^x	5	119	92	142	167
	10	190	115	192	234
	20	331	179	309	314
	30	471	213	368	400
	40	509	323	428	510
	60	890	280	736	968
L_w^x	5	38	68	57	63
	10	34	67	63	66
	20	24	64	59	60
	30	18	66	47	61
	40	15	89	48	52
	60	16	114	38	76

Figure 9 shows the variations of L_u^x and L_v^x with

different segment lengths T normalized by 3600 s, with L_u^x and L_v^x normalized by L_u^x (3600) and L_v^x (3600), respectively. The best fitting curves obtained by the least square method are shown as

$$\frac{L_u^x(T)}{L_v^x(3600)} = 0.90T/3600 + 0.10,$$

$$\frac{L_v^x(T)}{L_v^x(3600)} = 0.86T/3600 + 0.14, \qquad (18)$$

where T is the average segment length in seconds. This indicates a good linear relationship between the normalized L_u^x and the segmeant length T. As expected, Fig. 9a is comparable to the result of Yu et al. (2008).

Figure 10 shows variations of turbulence integral scale calculated based on 10-min segment with mean wind speed for Typhoon Damrey. It demonstrates that all the longitudinal, lateral, and vertical turbulence scales (L_u^x, L_v^x, and L_w^x) increase with mean wind speed in general, especially with the wind speed higher than 16 m s^{-1}. The vertical integral scale L_w^x, with a relatively small deviation, shows comparatively high sensitivity to the mean wind speed, while the lateral integral scale L_v^x changes a little with the increasing wind speed.

Figure 11 illustrates that all the 10-min turbulence integral scales decrease with TI. The scattered points, with the ranges of about 500, 200, and 100 m of the longitudinal, lateral, and vertical integral scales, respectively, imply a highly dispersed distribution. It can also be seen that L_u^x and L_w^x decrease evidently in the case that I is < 0.16.

4. Conclusions

Using high resolution data observed from different sites in southern China during four typhoon passages, a thorough analysis of the gust factor and turbulence integral scale characteristics was performed. The results are concluded as follows:

(1) The gust factor decreases with increase of the gust duration, and decreases more rapidly in rougher regimes.

(2) In general, the gust factor decreases with the mean wind speed, but will not change if the mean wind speed is higher than a critical value, which is suggested to be 14 m s^{-1} (Mitsuta and Tsukamoto, 1989) under a relative smooth and homogeneous upstream terrain condition. When it comes to rough and inhomogeneous conditions, the critical value will be larger than 14 m s^{-1}.

(3) The gust factor is sensitive to roughness

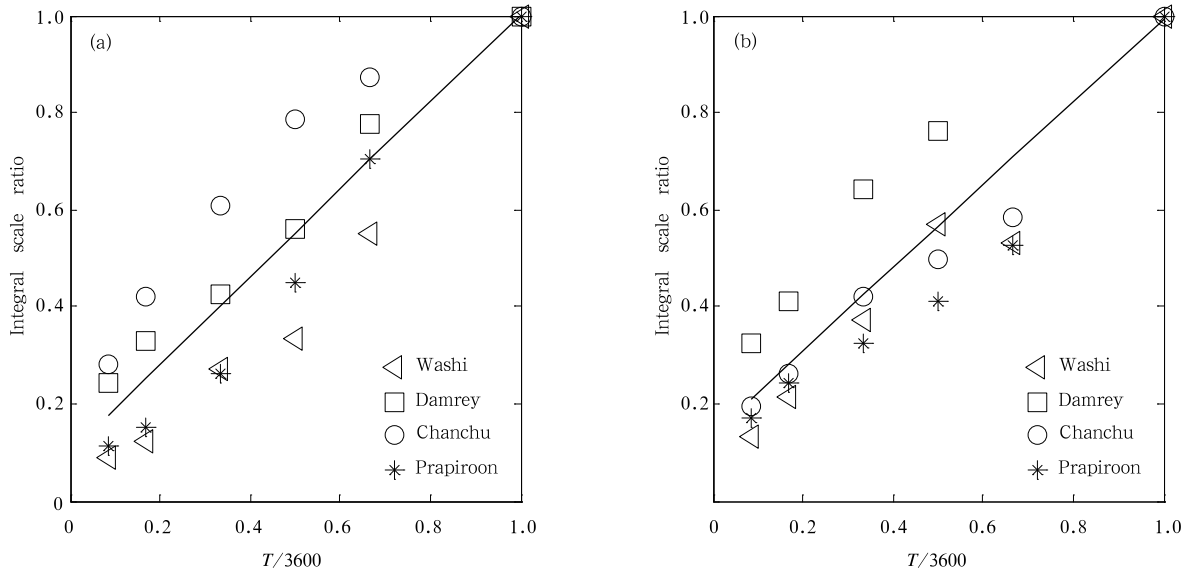

Fig. 9. Integral length scale ratios of (a) $L_u^x(T)/L_u^x(3600)$ and (b) $L_v^x(T)/L_v^x(3600)$ vs. the record length ratio $T/3600$.

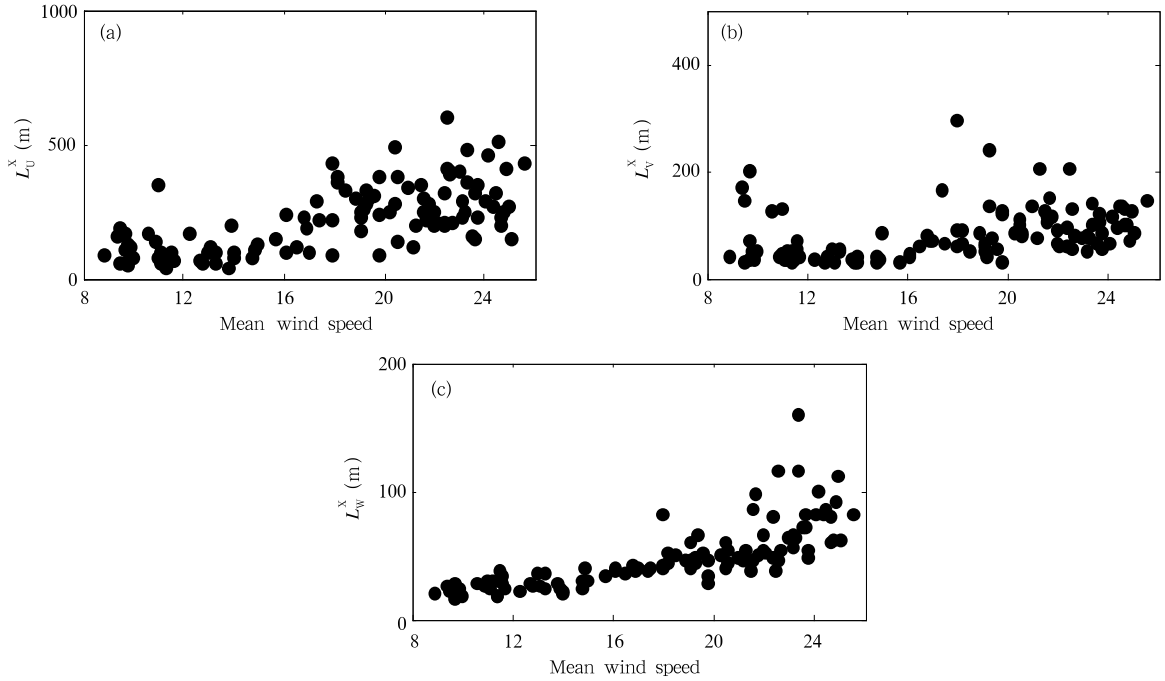

Fig. 10. Variations of turbulence integral scale with the (a) longitudinal, (b) lateral, and (c) vertical components of the mean wind for Typhoon Damrey.

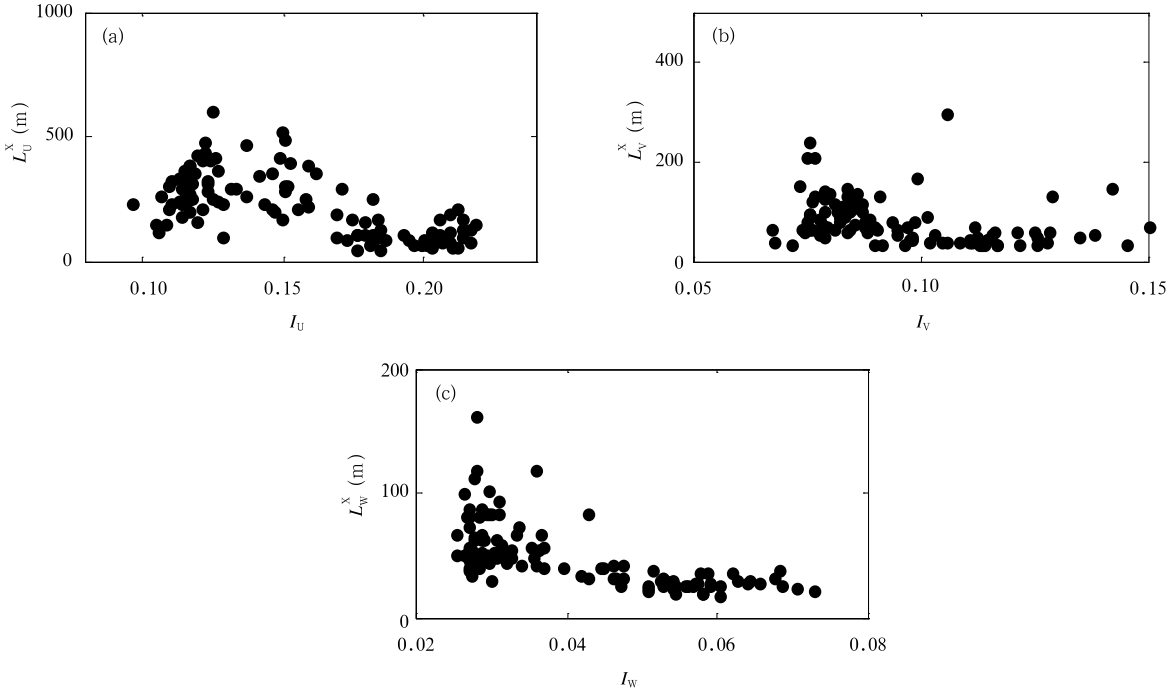

Fig. 11. Variations of turbulence integral scale with the (a) longitudinal, (b) lateral, and (c) vertical components of the turbulence intensity for Typhoon Damrey.

length. On the whole, the gust factor increases approximately linearly with roughness length. The 2-s/10-min gust factors are 1.29, 1.33, 1.42, 1.51, and 1.57, respectively, for the sea, smooth, open, open to roughly open, and roughly open to rough regime.

(4) The relationship between the gust factor and

TI can be described as: $G = 1 + \alpha I$. The constant α, usually called the peak factor, is different from typhoon to typhoon due to different roughness characteristics. The values of α are 2.28, 2.42, 2.96, and 2.09, respectively for typhoons Washi, Damrey, Chanchu, and Prapiroon.

(5) The autocorrelation coefficient, longitudinal and lateral turbulence integral scales increase with the segment length. The vertical turbulence integral scale is much smaller than the longitudinal and lateral ones, and changes a little with the segment length. The 10-m longitudinal integral scale ranges from 134 to 287 m, while the 60-min longitudinal integral scale changes from 678 to 1105 m. It seems that 10 and 60-min integral scales are not in the same order. Only the ratio L_u^x/L_v^x in Typhoon Damrey, with a value of 2.5, is comparable to previous results.

(6) The longitudinal, lateral, and vertical turbulence integral scales increase with the mean wind speed, and decrease with the turbulence intensity.

From the above discussion, it follows that proper and thorough analysis of turbulence characteristics of typhoons in South China may help with the design and risk evaluation of tall buildings in prevention of future typhoon attacks.

Acknowledgments. We wish to thank Professor Song Lili for providing the analyzed data. Thanks also go to the three anonymous reviewers for their valuable comments.

REFERENCES

Beljaars, A. C. M., 1987: The measurement of gustiness at routine wind stations—-A review. KNMI Scientific Rep., WR87-11, 5.

Brasseur, O., 2001: Development and application of a physical approach to estimating wind gusts. *Mon. Wea. Rev.*, **129**, 5–25

Cao, S., Y. Tamura, N. Kikuchi, M. Saito, I. Nakayama, and Y. Matsuzaki, 2009: Wind characteristics of a strong typhoon. *J. Wind. Eng. Ind. Aerod.* **97**(1), 11–21.

Choi, E. C. C., 1983: *Wind Loading in Hong Kong: Commentary on the Code of Practice on Wind Effects Hong Kong.* Hong Kong Institution of Engineers, Hong Kong, 23–26.

——, 1999: Extreme wind characteristics over Singapore–an area in the equatorial belt. *J. Wind. Eng. Ind. Aerod*, **83**(1–3), 61–69.

——, and F. A. Hidayat, 2002: Gust factors for thunderstorm and non-thunderstorm winds. *J. Wind. Eng. Ind. Aerod.* **90**(12–15), 1683–1696.

Davis, F., and H. Newstein, 1968: The variation of gust factors with mean wind speed and with height. *J. Appl. Meteor.*, **7**, 372–378.

Faber, S. E., and G. J. Bell, 1963: Typhoons in Hong Kong and building design. The Engineering Society of Hong Kong, 28 pp.

Flay, R. G. J., and D. C. Stevenson, 1988: Integral length scales in strong winds below 20 m. *J. Wind. Eng. Ind. Aerod.*, **28**, 21–30.

Floris, C., and L. D. Iseppi, 1998: The peak factor for gust loading: A review and some new proposals. *Meccanica*, **33**(3), 319–330.

Fu, J. Y., Q. S. Li, J. R. Wu, Y. Q. Xiao, and L. L. Song, 2008: Field measurements of boundary layer wind characteristics and wind-induced responses of super-tall buildings. *J. Wind. Eng. Ind. Aerod.*, **96**(8–9), 1332–1358.

Garg, R. K., J. X. Lou, and M. Kasperski, 1997: Some features of modeling spectral characteristics of flow in boundary layer wind tunnels. *J. Wind Eng. Ind. Aerod.*, **72**, 1–12.

Goyette, S., O. Brasseur, and M. Beniston, 2003: Application of a new wind gust parameterization: Multiscale case studies performed with the Canadian regional climate model. *J. Geophys. Res.*, **108**(D13), 4374, doi: 10.1029/2002JD002646.

Harikrishna, P., J. Shanmugasundaram, S. Gomathinayagam, and N. Lakshmanan, 1999: Analytical and experimental studies on the gust response of a 52-m tall steel lattice tower under wind loading. *Comput. Struct.*, **70**(2), 149–160.

Harstveit, K., 1996: Full scale measurements of gust factors and turbulence intensity, and their relations in hilly terrain. *J. Wind. Eng. Ind. Aerod.*, **61**(2–3), 195–205.

Højstrup, J., 1993: A statistical data screening procedure. *Meas. Sci. Technol.*, **4**(2), 153–157.

Hsu, S. A., 2003: Estimating overwater friction velocity and exponent of power-law wind profile from gust factor during storms. *J. Waterw. Port. C-asce.*, **129**(4), 174–177.

——, and B. W. Blanchard, 2004: Estimating overwater turbulence intensity from routine gust-factor measurements. *J. Appl. Meteor.*, **43**(12), 1911–1916.

Hui, M. C. H., A. Larsen, and H. F. Xiang, 2009: Wind turbulence characteristics study at the Stonecutters Bridge site. Part I: Mean wind and turbulence intensities. *J. Wind. Eng. Ind. Aerod.*, **97**(1), 22–36.

Jiang, X. P., Z. Zhong, and C. X. Liu, 2008: The effect of typhoon-induced SST cooling on typhoon intensity: The case of Typhoon Chanchu (2006). *Adv. Atmos. Sci.*, **25**(5), 1062–1072, doi: 10.1007/s00376-008-1062-9.

Johnson, H. K., J. Højstrup, H. J. Vested, and S. E. Larsen, 1998: On the dependence of sea surface roughness on wind waves. *J. Phys. Oceanogr.*, **28**(9), 1702–1716.

Jungo, P., S. Goyette, and M. Beniston, 2002: Daily wind gust speed probabilities over Switzerland according to three types of synoptic circulation. *Int. J. Climatol.*, **22**(4), 485–499.

Kato, N., T. Ohkuma, J. R. Kim, H. Marukawa, and Y. Niihori, 1992: Full scale measurement of wind velocity in two urban areas using an ultrasonic anemometer. *J. Wind. Eng. Ind. Aerod.*, **41**(1–3), 67–78.

Krayer, W. R., and R. D. Marshall, 1992: Gust factors applied to hurricane winds. *Bull. Amer. Meteor. Soc.*, **73**, 613–617.

Kobayashi, H., A. Hatanaka, and T. Ueda, 1994: Active simulation of time histories of strong wind gust in a wind-tunnel. *J. Wind. Eng. Ind. Aerod.*, **53**(3), 315–330.

Letchford, C., A. Gardner, R. Howard, and J. Schroeder, 2001: A comparison of wind prediction models for transitional flow regimes using full-scale hurricane data. *J. Wind. Eng. Ind. Aerod.*, **89**(10), 925–945.

Li Qingqing, Duan Yihong, Fu Gang, and Yu Hui, 2009: A numerical investigation of the eyewall evolution of a tropical cyclone. *Acta Meteor. Sinica*, **23**(5), 517–538.

Li, Q. S., Y. Q. Xiao, C. K. Wong, and A. P. Jeary, 2004: Field measurements of typhoon effects on a super tall building. *Eng. Struct.*, **26**(2), 233–244.

Liu, S. H., F. Hu, H. Liu, et al., 2003: Turbulence length scales, dissipation rates and structure parameters above the forest canopy. *Acta Scicentiarum Naturalum Universitis Pekinesis*, **39**, 73–82. (in Chinese)

Ming, J., Y. Q. Ni, and X. Y. Shen, 2009: The dynamical characteristics and wave structure of Typhoon Rananim (2004). *Adv. Atmos. Sci.*, **26**(3), 523–542, doi: 10.1007/s00376-009-0523-0.

Mitsuta, Y., 1962: Gust factor and analysis time of gust. *J. Meteor. Soc. Japan*, **40**, 242–244.

—— and O. Tsukamoto, 1989: Studies on spatial structure of wind gust. *J. Appl. Meteor.*, **28**, 1155–1160.

Miyata, T., H. Yamada, H. Katsuchi, and M. Kitagawa, 2002: Full-scale measurement of Akashi-Kaikyo Bridge during typhoon. *J. Wind. Eng. Ind. Aerod.*, **90**(12–15), 1517–1527.

Nielsen, N. W., and C. Petersen, 2001: Calculation of wind gusts in DMI-HIRLAM. Danish Meteorological Institute Scientific Report, No. 01–03, 38.

Paulsen, B. M., and J. L. Schroeder, 2005: An examination of tropical and extratropical gust factors and the associated wind speed histograms. *J. Appl. Meteor.*, **44**(2), 270–280.

Powell, M. D., 1982: The transition of the Hurricane Frederic boundary-layer wind field from the open Gulf of Mexico to landfall. *Mon. Wea. Rev.*, **110**(12), 1912–1932.

Reed, D. A., and R. H. Scanlan, 1984: Autoregressive representation of longitudinal, lateral, and vertical turbulence spectral. *J. Wind. Eng. Ind. Aerod.*, **17**, 199–214.

Schroeder, J. L., D. A. Smith, and R. E. Peterson, 1998: Variation of turbulence intensities and integral scales during the passage of a hurricane. *J. Wind. Eng. Ind. Aerod.*, **77**, 65–72.

——, M. R. Conder, and J. R. Howard, 2002: Additional Insights into Hurricane Gust Factors. 25th Conference on Hurricanes and Tropical Meteorology, San Diego, CA, Amer. Meteor. Soc., P1.25.

——, and D. A. Smith, 2003: Hurricane Bonnie wind flow characteristics as determined from WEMITE. *J. Wind. Eng. Ind. Aerod.*, **91**(6), 767–789.

Sharma, R. N., and P. J. Richards, 1999: A re-examination of the characteristics of tropical cyclone winds. *J. Wind. Eng. Ind. Aerod.*, **83**(1-3), 21–33.

Shiau, B. S., 2000: Velocity spectra and turbulence statistics at the northeastern coast of Taiwan under high-wind conditions. *J. Wind. Eng. Ind. Aerod.*, **88**(2–3), 139–151.

Smedman, A. S., H. Bergström, and U Högström, 1995: Spectra, variances and length scales in a marine stable boundary layer dominated by a low level jet. *Bound.-Layer Meteor.*, **76**(3), 211–232.

Sozzi, R., M. Favaron, and T. Georgiadis, 1998: Method for estimation of surface roughness and similarity function of wind speed vertical profile. *J. Appl. Meteor.*, **37**(5), 461–469.

Vickers, D., and L. Mahrt, 1997: Quality control and flux sampling problems for tower and aircraft data. *J. Atmos. Oceanic Tech.*, **14**(3), 512–526.

Vickery, P. J., and P. F. Skerlj, 2005: Hurricane gust factors revisited. *J. Struct. Eng-ASCE*, **131**(5), 825–832.

Wieringa, J., 1976: An objective exposure correction method for average wind speeds measured at a sheltered location. *Quart. J. Roy. Meteor. Soc.*, **102**, 241–253.

Wieringa, J., 1992: Updating the Davenport roughness classification. *J. Wind. Eng. Ind. Aerod.*, **41**(1–3), 357–368.

Xu, Y. L., and S. Zhan, 2001: Field measurements of Di Wang Tower during Typhoon York. *J. Wind. Eng. Ind. Aerod.*, **89**(1), 73–93.

Yu, B., A. G. Chowdhury, and F. J. Masters, 2008: Hurricane wind power spectra, cospectra, and integral length scales. *Bound.-Layer Meteor.*, **129**(3), 411–430.

Yuan Jinnan, Lin Ailan, and Liu Chunxia, 2009: Spatial and temporal variations of tropical cyclones at different intensity scales over the western North Pacific from 1945 to 2005. *Acta Meteor. Sinica*, **23**(5), 550–561.

Zhang, H., J. Chen, and S. U. Park, 2001: Turbulence structure in unstable conditions over various surfaces. *Bound.-Layer Meteor.*, **100**(2), 243–261.

Zhao Yu, Cui Xiaopeng, and Wang Jianguo, 2009: A study on a heavy rainfall event triggered by an inverted typhoon trough in Shandong Province. *Acta Meteor. Sinica*, **23**(4), 465–484.

Zhou, M. Y., H. Hsu, and Y. Yuan, 2003: Mesoscale numerical simulation of the developing process of cyclones moving to the Yellow Sea and East China Sea. *Chinese J. Geophys.*, **46**, 175–178. (in Chinese)